Proceedings of the IASTED International Conference
Signal and Image Processing (SIP'98)
October 28–31, 1998, Las Vegas, Nevada

Wavelet Transform Compression of Functional Magnetic Resonance Image Sequences

Carl Taswell
UCSD School of Medicine, La Jolla, CA 92093-0603
Computational Toolsmiths, Stanford, CA 94309-9925

Abstract

Image sequences from functional neuroimaging experiments with 3-D magnetic resonance scans of the human brain were wavelet transformed using a variety of orthogonal and biorthogonal wavelet filters with different treatments of the image borders. Contrary to the expectation that higher-order wavelets with more sophisticated boundary treatments would yield better compression, simple Haar wavelets without any boundary treatment provided the best compression throughout the rate-distortion performance curve.*

Keywords: medical imaging, FMRI sequences, wavelet transforms.

1 Introduction

Biorthogonal wavelet filters [1] with convolutions incorporating symmetric reflection at the image borders [2] have achieved significant success in important applications such as the FBI fingerprint image compression standard [3] and continue to receive attention in imaging studies [4]. The development of boundary treatments with orthogonal wavelet filters [5] and the continuing use of orthogonal cubic spline wavelets [6] in imaging applications provide other examples of methods that might be termed "sophisticated" when compared with simple Haar wavelets which preclude the need for any boundary treatment.

Indeed, the popularity of the more sophisticated methods might lead one to think that analysis with simple Haar wavelets is no longer necessary or appropriate. However, this report provides an important counter-example in the application field of functional neuroimaging with magnetic resonance scans where Haar wavelets easily outperformed the more sophisticated alternatives. Lower levels of distortion for fixed rates of data compression were achieved throughout most of the rate-distortion performance curve for Haar wavelets when compared with the alternatives.

2 Methods

Wavelet filter families are named and indexed here according to the conventions established in [7]. The extended families Daubechies Real Biorthogonal Least Uncertain (DRBLU) and Daubechies Real Orthogonal Least Asymmetric (DROLA) include the lower-order filters originally defined in [1] and [8], respectively. For the treatment of boundaries, the convolution types "SRS" and "BAF" implement the symmetrically reflected signal algorithm of Brislawn [2] and the boundary adjusted filter algorithm of Cohen Daubechies and Vial [5], respectively. Experimental results reported here were computed with Version 4.5a2 of the WAVBOX Software Library [9] running in Version 5.1.0 of the MATLAB technical computing environment [10] on a Toshiba Tecra 720CDT.

Functional magnetic resonance image (FMRI) sequences from functional neuroimaging experiments were kindly provided by Dr. Greg Brown of the UCSD Department of Psychiatry. These 4-D brain scan sequences consisted of $T > 100$ time samples of 3-D spatial volumes discretized

*Paper 281-162.

at $64 \times 64 \times 8$ voxel resolution (considered to be 8 slices of 64×64 pixel images). For the example results shown here, there were $T = 146$ time points in the sequence.

The experiment for results reported in Table 1 and Figure 1 was performed using a 2 level 2-D discrete wavelet transform (DWT) on the image slices $I[j,k]$ with the indicated filter and convolution. Estimates $\hat{I}[j,k]$ were reconstructed with a fraction $0 < f \leq 1$ of the most significant wavelet transform coefficients. Signal-to-noise ratios were computed as

$$\mathrm{SNR} = 10 \log 10 \frac{\sum_{j,k} |I[j,k]|^2}{\sum_{j,k} |I[j,k] - \hat{I}[j,k]|^2}$$

with results averaged over all images and reported as mean decibels (dB).

The experiment reported in Figure 2 was performed analogously using a 2 level 3-D DWT on the spatial volumes. For the density and distribution of 3-D transform coefficients, the probability density function (PDF) was estimated with a 25-point probability mass function (25-bin histogram), and the cumulative distribution function (CDF) was estimated with a 101-point quantile curve (101 percentiles at $0.00, 0.01, \ldots, 1.00$).

3 Results

Table 1 presents results expressed as mean SNR values for a compression experiment measuring distortion as a function of 4 fixed compression rates at $f = 0.1$, 0.2, 0.4, and 0.8 which yield a performance range from low to high SNR. Standard deviations were approximately 1% of means at the highest SNR values, and 2-4% at the lowest SNR values.

The real orthogonal Haar filters, which do not require any special boundary treatment in the implementation of the convolution, performed better than the next closest filter-convolution combination, DROLA(8;4) filters with CPS convolution. The difference was approximately 0.5 dB better at $f = 0.8$ and $f = 0.4$, 0.1 dB better at $f = 0.2$, and 0.1 dB worse only at the lowest rate $f = 0.1$ where the discrepancy was considered insignificant because it was the same as the standard deviations.

At the lowest order of wavelet, all families reduce to the Haar wavelet. Thus, DRBLU(2,2;1,1) and DROLA(2;1) are equivalent to Haar. Figure 1 displays the rate-distortion performance curves for the DRBLU$(N_a, N_s; K_a, K_s)$ family with $K_a = K_s \equiv K$ for $K = 1, \ldots, 5$. Error bars in these curves correspond to ± 1 standard deviation. Again, the Haar wavelet (top-most curve) performs best throughout the range of the rate-distortion curves.

Finally, Figure 2 displays estimates of the PDF and CDF for the 3-D DWT coefficients computed with the Haar filter averaged over all spatial volumes in the time sequence. The dashed curve with error bars on the points for the PDF is plotted as the mean probabilities at the midpoints of the histogram bins for the transform coefficient values. The solid curve for the CDF is plotted as the cumulative probabilities (or quantile levels) at the coefficient quantile values. Standardized skewness and kurtosis coefficients for the distribution were calculated to be 3.03 and 32.5, respectively, with a longer tail to the right and significant leptokurtosis. Mean SNR for the 3-D compression was 5.04, 8.92, 17.1, and 35.7 dB at the 4 compression rates of $f = 0.1$, 0.2, 0.4, and 0.8, respectively. Standard deviations were ≤ 0.2 dB at all 4 rates.

4 Conclusion

Results from rate-distortion analyses of compression experiments with imaging sequences from functional brain scans demonstrated that no benefit could be obtained with any of the higher-order wavelets or more sophisticated boundary treatments when compared with the simple Haar wavelet. Since the Haar wavelet does not require any special boundary treatment, it lends itself readily to compression in the third spatial dimension which has a resolution of only 8 grid points when compared with the first 2 dimensions for the image slices which have a resolution grid of 64×64. Moreover, because the Haar filter has only 2 filter taps, data compression with the 3-D Haar DWT provides the most efficient method from the perspective of computational complexity. This initial

study has demonstrated clear advantages of the Haar wavelet for compression of FMRI sequences. However, future research must establish whether or not the compression preserves the fidelity of critical information. In other words, can spatial regions of "functional activity" be detected in the time sequence with sufficient accuracy both before and after the data compression and reconstruction transforms?

References

[1] Albert Cohen, Ingrid Daubechies, and J. C. Feauveau. Biorthogonal bases of compactly supported wavelets. *Communications on Pure and Applied Mathematics*, 45:485–560, 1992.

[2] Christopher M. Brislawn. Classification of nonexpansive symmetric extension transforms for multirate filter banks. *Applied and Computational Harmonic Analysis*, 3(4):337–357, October 1996.

[3] T. Hopper, Jonathan N. Bradley, and Christopher M. Brislawn. WSQ gray-scale fingerprint image compression specification. Technical Report IAFIS-IC-0110v2 (rev. 2.0), Federal Bureau of Investigation, February 1993.

[4] Antonin Chambolle, Ronald A. DeVore, Nam-yong Lee, and Bradley J. Lucier. Nonlinear wavelet image processing: Variational problems, compression, and noise removal through wavelet shrinking. *IEEE Transactions on Image Processing*, 7(3):319–335, March 1998.

[5] Albert Cohen, Ingrid Daubechies, and Pierre Vial. Wavelets on the interval and fast wavelet transforms. *Applied and Computational Harmonic Analysis*, 1(1):54–81, December 1993.

[6] Stéphane G. Mallat and Frédéric Falzon. Analysis of low bit rate image transform coding. *IEEE Transactions on Signal Processing*, 46(4):1027–1042, April 1998.

[7] Carl Taswell. *The Systematized Collection of Wavelet Filters Computable by Spectral Factorization of the Daubechies Polynomial*. Computational Toolsmiths, `www.toolsmiths.com`, 1997.

[8] Ingrid Daubechies. Orthonormal bases of compactly supported wavelets: II. variations on a theme. *SIAM Journal on Mathematical Analysis*, 24(2):499–519, March 1993.

[9] Carl Taswell. *WAVBOX Software Library and Reference Manual*. Computational Toolsmiths, `www.wavbox.com`, 1993–98.

[10] The MathWorks, Inc., Natick, MA. *MATLAB The Language of Technical Computing: MATLAB 5.1 New Features*, May 1997.

Table 1: Mean SNR in dB for 2-D DWT Compression of FMRI Sequence

Filter and Convolution		$f = 0.1$	$f = 0.2$	$f = 0.4$	$f = 0.8$
DRBLU(5,3;2,2)	SRS	3.9046	7.5107	15.7507	34.3805
DRBLU(8,4;3,3)	SRS	2.7493	5.5690	13.2720	31.9230
DRBLU(9,7;4,4)	SRS	4.4189	8.1333	16.1666	34.8983
DRBLU(10,10;5,5)	SRS	2.8034	6.2204	13.7847	32.4608
DROLA(2;1)=Haar	—	4.4952	8.4525	16.7452	35.7085
DROLA(4;2)	BAF	4.4851	8.2178	16.0479	34.9107
DROLA(6;3)	BAF	4.5104	8.1591	15.8193	34.6766
DROLA(8;4)	BAF	4.5297	8.2442	15.9418	34.9638
DROLA(4;2)	CPS	4.4772	8.2473	16.0893	35.0742
DROLA(6;3)	CPS	4.5505	8.2769	16.0779	35.0327
DROLA(8;4)	CPS	4.5847	8.3692	16.1918	35.1858

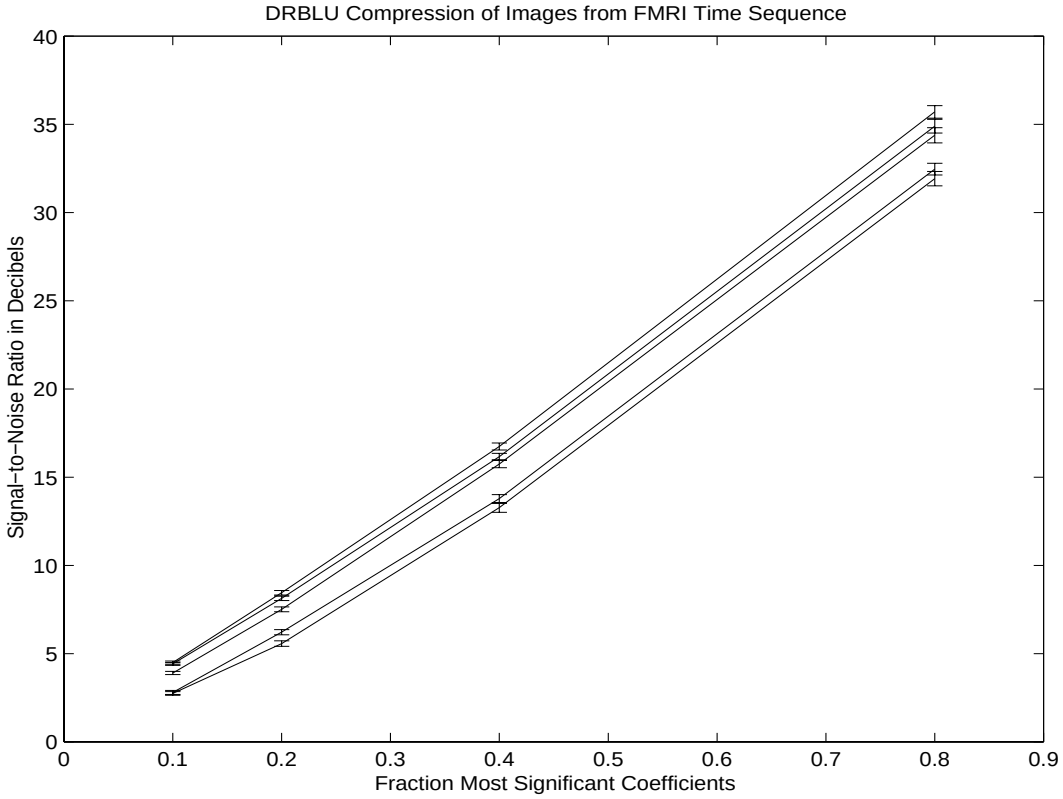

Figure 1: Mean SNR for 2-D DRBLU DWT Compression of FMRI Sequence.

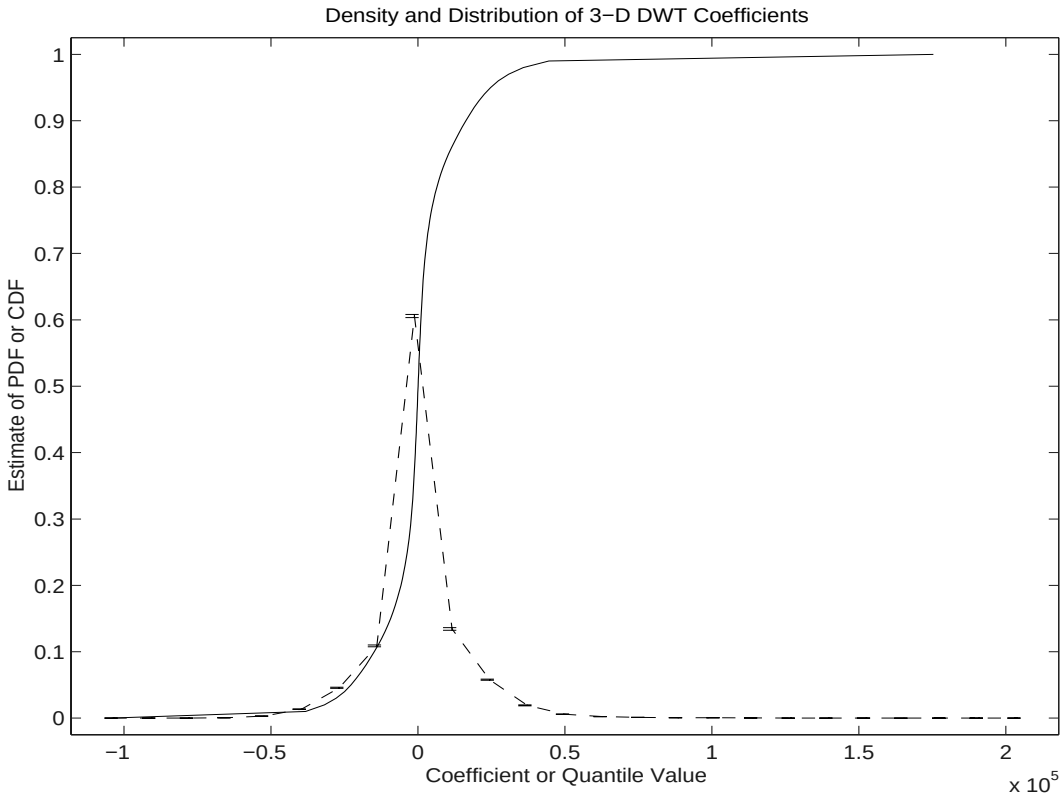

Figure 2: PDF and CDF for 3-D Haar DWT Coefficients for FMRI Sequence.